Journal of Membrane Science, Volume 720, March 2025, Article number 123784
DOI:10.1016/j.memsci.2025.123784

Exploring advanced and sustainable bioaugmentation-enhanced ultrafiltration processes for the removal of emerging contaminants

Tingming Ye[a, c, d], QingJi Wang [c, d], Jing Qi[a, e], Baiwen Ma[a, e, *], Tao Lyu[f], Chengzhi Hu[a, e], Mathias Ulbricht[g], Huijuan Liu[b]

[a] Key Laboratory of Drinking Water Science and Technology, Research Center for Eco-Environmental Sciences, Chinese Academy of Sciences, Beijing 100085, China
[b] Center for Water and Ecology, State Key Joint Laboratory of Environment Simulation and Pollution Control, School of Environment, Tsinghua University, Beijing 100084, China
[c] CNPC Research Institute of Safety and Environment Technology, Beijing 102206, China
[d] State Key Laboratory of Petroleum Pollution Control, Beijing 102206, China
[e] University of Chinese Academy of Sciences, Beijing 100049, China
[f] Faculty of Engineering and Applied Sciences, Cranfield University, College Road, Bedfordshire MK43 0AL, UK
[g] Lehrstuhl für Technische Chemie II, Universität Duisburg-Essen, Essen 45117, Germany

* Corresponding author. Email address: bwma@rcees.ac.cn

Abstract: The development of cost-effective and sustainable water treatment technologies is crucial for supporting the water sector and the public in achieving global sustainable development goals (SDG 6) and carbon neutrality targets. Ultrafiltration (UF), known for its compactness, relatively high performance, and ease of operation, has been widely deployed in water treatment. However, its limitations in removing some emerging contaminants (ECs) and membrane fouling issues have hindered its broader application. This study investigated the incorporation of bioaugmented filtration into conventional UF processes to enhance ECs removal and mitigate membrane fouling during the treatment of real drinking water sources. In addition to effectively removing microorganisms (eukaryotes and bacteria), polysaccharides (13.9%), and inorganic pollutants ($CaCO_3$, MgO, SiO_2, and Al_2O_3), the proposed approach also demonstrated superior removal (4.6%-100.0%) of four target ECs (atenolol, carbamazepine, trimethoprim, and sulfamethoxazole) compared to direct UF process (1.5%-47.5%). After 56 days of operation, the bioaugmented pre-treatment significantly reduced transmembrane pressure (TMP) by 80.2% compared to the direct UF process. Mechanisms studies further reassured that ECs removal followed oxidation during bioaugmentation pre-treatment. The time-of-flight secondary ion mass

Published by Elsevier. This is the Author Accepted Manuscript issued with: Creative Commons Attribution License (CC:BY 4.0).
The final published version (version of record) is available online at DOI:10.1016/j.memsci.2025.123784. Please refer to any applicable publisher terms of use.

spectrometry with in-depth analysis capability (around 5 nm) revealed that the UF membrane primarily removed atenolol through adsorption. The toxicity prediction results of typical ECs and their degradation intermediates indicated a significant reduction in ecological risk for most intermediates. The findings from this work demonstrate the feasibility of using low-carbon and few-chemical water treatment technologies to secure drinking water quality.

Keywords: Low-carbon and few-chemical technology, Bioaugmented filtration, Ultrafiltration, Emerging contaminants removal, Membrane performance

1. Introduction

With the introduction of Zero-Pollution Action Plan and Carbon Neutrality targets to be achieved in 2050, cost-effective water treatment technologies with low carbon footprints are crucial for the water sector to support these global goals (Qu and Chen, 2024). However, increasing anthropogenic activities are exacerbating water resource pollution, putting greater pressure on widely adopted water treatment infrastructures (Wei et al., 2023). Amongst these emerging challenges, emerging contaminants (ECs) have posed significant difficulties in terms of effective removal due to their recalcitrant nature (Marques et al., 2024). Those ECs consists of a wide range of organic chemical compounds, including persistent organic pollutants, endocrine-disrupting compounds, and pharmaceutical and personal care products (Palaniswamy et al., 2024; Wang et al., 2023). In the environment, ECs typically exist at trace levels, but can still cause significant health issues for human and wildlife. Long-term consumption of water containing ECs may lead to imbalances in intestinal flora, potentially affecting the body's immune system, liver and kidney function, and contributing to the onset of chronic diseases or cancer (Dirani et al., 2024). Traditional water treatment technologies, such as coagulation and oxidation, are often ineffective in removing these ECs (Chen et al., 2024; Zhao et al., 2024). Therefore, there is an urgent need to develop water treatment technologies coupling with low carbon characteristic to tackle these challenges.

Numerous efforts have been made to effectively remove ECs in water treatment, including the ozone-activated carbon treatment approach (Huang et al., 2018), producing high-quality water for end users. However, the process requires chemical inputs, which are less desirable as they contribute to indirect carbon emissions. Some biological remediation methods (e.g. biofiltration) and physical separation techniques (e.g. membrane filtration) have also been deployed and are deemed as low-carbon approaches for water treatment (Xu et al., 2021). These processes are pivotal in addressing various contaminants, including pathogenic bacteria, while minimizing resource consumption and operational complexity (Ajaz et al., 2024; Yang et al., 2024). In terms of the removal of ECs, the incorporated bioremediation and membrane filtration approach offers theoretical potential but requires further exploration.

Biofiltration reactors can support the growth of diverse functional microbial communities, facilitating the biodegradation and biotransformation of ECs into harmless or less toxic substances (Zhou et al., 2022). Among the microorganisms in these biofilms, manganese-oxidizing bacteria have attracted significant attention for their ability to remove Mn^{2+} from water and produce biological manganese oxide, which possesses exceptional adsorption and oxidation properties (Bai et al., 2016). Numerous studies have demonstrated the remarkable efficacy of biological manganese oxides in removing recalcitrant ECs (Furgal et al., 2015; Ren et al., 2023). Therefore, inoculating manganese-oxidizing bacteria into biofiltration systems as a bioaugmented filtration technology represents an ecologically and economically viable strategy to enhance water purification (Therdkiattikul et al., 2023). However, the scouring action of water can inevitably detach biofilm from the filter material, potentially introducing microorganisms into the effluent (Bai et al., 2024). Therefore, combining this approach with subsequent membrane technology is an appropriate strategy to maintain water quality and safety.

Although nanofiltration membranes with extremely small pore sizes can provide high quality effluent, the high operational and energy cost remain significant barriers. Ultrafiltration (UF) membranes, on the other hand, are still the most widely applied

technology for drinking water treatment globally. However, membrane fouling is inevitable, particularly due to natural organic matters and microorganisms (Meng et al., 2020), resulting in degraded membrane performance and increased operational costs. In addition, UF is insufficient for effectively removing most ECs due to its relatively larger membrane pore size (Urtiaga et al., 2013). Previous researches found biofiltration as a pre-treatment could decrease irreversible UF membrane fouling by up to 68% (Andrews et al., 2015; Huck et al., 2014), and UF can effectively reject the majority of microorganisms present in biofiltration effluent (Mohammed et al., 2021). Furthermore, the upstream biological treatment of ECs can lead to a reduced load on UF membranes and theoretically improve micropollutant removal efficiency. The proposed bioaugmentation using manganese-oxidizing bacteria also has the potential to further aid in the removal of toxic metals (e.g., Mn^{2+}) during water treatment. This integrated process holds considerable practical significance for water treatment due to its potential high efficiency and low maintenance (Liu et al., 2023). However, the overall performance and underlying mechanisms remain largely unexplored.

This study aims to investigate the performances and mechanisms of integrating bioaugmented filtration with membrane UF processes for water treatment, with a particular focus on the removal of emerging micropollutants and systems sustainability (e.g. membrane fouling). Four commonly occurring ECs, i.e. atenolol (ATL), carbamazepine (CBZ), trimethoprim (THP), and sulfamethoxazole (SMX), were selected as model pollutants (Manoli et al., 2022), and river water was used as the base water source. Additionally, the toxicity characteristics of both parent compounds and intermediates formed during bioaugmented filtration were assessed to evaluate potential risks in the final effluent. UF membrane performance was also evaluated based on changes in TMP, with comparisons made between biofouling, organic fouling, and inorganic fouling characteristics. These findings are anticipated to offer scientific foundation and technical support for the practical implementation of the proposed bioaugmented filtration-UF water treatment approach.

2. Materials and methods

2.1 Chemicals

Atenolol (98%) was purchased from Shanghai Aladdin Biochemical Technology Co., Ltd. (China). Carbamazepine (99%), trimethoprim (98%), and sulfamethoxazole (98%) were purchased from Shanghai Macklin Biochemical Technology Co., Ltd. (China). All other chemicals such as $Na_2HPO_4 \cdot 12H_2O$, KH_2PO_4, and $MnCl_2 \cdot 4H_2O$, were of analytical reagent grade and were purchased from Sinopharm Chemical Reagent Co., Ltd. (China). Ultrapure water was obtained from a Milli-Q water purification system (Millipore, USA).

2.2 Experimental set-up

The filter material for the reactor of bioaugmented filtration column (denoted as R, inside diameter is 10 cm and height is 1.5 m) utilized manganese sand (Ø 0.6-2 mm) sourced from a drinking water treatment plant in Inner Mongolia Province, China. During the culture stage (30 days), the reactor was inoculated with manganese-oxidizing bacteria QJX-1 (Ye et al., 2023). A hollow fiber UF membrane module (the effective membrane area is 0.02 m^2) was used as the subsequent treatment, operated at a flux of 8.3 L/(m^2·h), with a peristaltic pump programmed to reverse every 29 min of operation for 1 min, backwashing the membrane at a flux of 16.6 L/(m^2·h). The control group underwent direct ultrafiltration, while in the experimental group (R-UF), the feed water was treated with the R column before ultrafiltration. Four ECs (1 μg/L each of ATL, CBZ, THP, and SMX) were added to the water of Yongding River in Beijing as feed water, and the total operation period was 56 days. From day 28 to day 56, 2.5 mg/L Mn^{2+} was added into the feed water to simulate the sudden contamination of the water source with heavy metal. Specific details regarding the construction of the experimental device can be found in Supporting Information (SI) Method S1. A schematic diagram of the experimental setup is shown in SI Fig. S2.

2.3 Water quality analysis

The turbidity of the influent and effluent was measured using a turbidimeter (WQZ-2000, INESA Physico-Optical, China). Dissolved organic matter (DOM) was

determined by size exclusion chromatography coupled with an organic carbon detector (SEC-OCD, SEC-TOC, Shimadzu, Japan). The TSK HW50 S SEC column (20 mm × 250 mm, Toyopearl) was used to separate DOM of different molecular weights. The mobile phase was 1.5 g/L $Na_2HPO_4 \cdot 2H_2O$ + 2.5 g/L KH_2PO_4 phosphate buffer with a flow rate of 1.0 mL/min and the sample injection volume was 500 μL. The relationship between molecular weight and retention time of the SEC column was calibrated using polyethylene glycol (PEG) standards with molecular weights of 0.2, 0.4, 1, 2, 4, 6, 10, and 20 kDa (Ji et al., 2022). Additional methods for water quality analysis are described in SI Method S3.

2.4 Analytical methods of ECs and intermediates

The concentrations of ATL, CBZ, THP, and SMX were measured using ultra performance liquid chromatography-tandem quadrupole mass spectrometry (UPLC-MS/MS, TSQ Altis, Thermo Fisher, USA). An ACQUITY UPLC® BEH C18 1.7 μm (2.1 × 50 mm) chromatographic column maintained at 35 ℃, was used for separation. The mobile phase consisted of 0.1% formic acid solution (A) and acetonitrile (B), with a flow rate of 0.3 mL/min. The gradient elution method was as follows: 0–0.5 min, 90% A, 0.5–6 min, 90%–40% A linearly, 6–7.5 min, 40% A, 7.5–8 min, 40%–90% A linearly, 8–11.5 min 90% A. The injection volume was 10 μL. The mass spectrometry (MS) parameters were as follows: ion spray voltage was set to 3500 V, the source temperature to 300 ℃, and detection was conducted in positive ion mode. The MS-MS parameters of ECs are provided in SI Table S1. The method for identification of the intermediates is provided in SI Method S4.

2.5 Toxicity prediction

Based on the quantitative structure-activity relationship (QSAR) methodologies, the Ecological Structure Activity Relationships (ECOSAR) program was utilized to predict the acute and chronic toxicities of ECs and identified intermediates. Additionally, the Toxicity Estimation Software Tool (T.E.S.T.) was used to predict bioconcentration factor, developmental toxicity, and mutagenicity.

2.6 Membrane characterization

The UF membrane surface after operation was deeply dissected by time-of-flight secondary ion mass spectrometry (ToF-SIMS, ToF-SIMS V, ION-TOF GmbH, Germany) with remarkable depth profiling capability to elucidate the three-dimensional (3D) structure of the UF membrane and cake layer. A 1.5 cm hollow fiber membrane was clipped and axially cut from one side. The membrane was then smoothed out and affixed face up onto a glass sheet. Paraffin wax was melted and poured into a stainless-steel mold (2 cm × 2 cm × 1 cm). Once cooled to a non-flowing state, the hollow fiber membrane attached to the glass sheet was gently pressed into the paraffin. The paraffin was then cut into 1.5 cm × 1.5 cm × 1 cm bulk samples. The prepared sample was placed on the ToF-SIMS sample table and sputtered using a 20 keV argon cluster ion beam within a 500 μm × 500 μm sputtering region. A 30 keV Bi^{3+} primary ion beam (pulse current was 1 pA) was utilized to analyze the sputtering region (analysis area was 100 μm × 100 μm). To compensate for sample charging, a low-energy electron neutralization gun was employed. Secondary ions and ion clusters were collected in positive ion mode. Data was processed using SurfaceLab 7 (ION-ToF) software. The signal intensity of characteristic secondary ions for analysis was normalized. Additionally, a 3D image of the sample was reconstructed based on depth analysis data. The characteristic ion of PVDF was m/z = 133 and that of ATL was m/z = 267 (Wu et al., 2021). Other characterization methods for UF membrane and cake layer are detailed in SI Method S5.

3. Results

3.1 Variation of TMP and membrane surface morphology

TMP plays an important role in UF membrane performance. As can be seen from Fig. 1a, the TMP was swiftly escalated to 21.2 kPa for direct UF process, while that of R-UF process was only increased to 3.2 kPa within 35 days. In the following 21 days, the TMP further slowly increased to 23.7 kPa at an average rate of 0.12 kPa/d, while the TMP of R-UF process further increased from 3.2 kPa to 4.7 kPa at an average rate of

0.07 kPa/d, respectively. After 56 days operation, the TMP of direct UF process was 5 times that of the R-UF process.

In comparison with TMP, UF membrane surface morphology also can visually reflect the effectiveness of pretreatment. The plane and profile of the membrane were analyzed by scanning electron microscopy (SEM, Fig. 1b-1e and SI Fig. S3). The SEM images revealed that the fresh membrane pores were evenly distributed (SI Fig. S3). However, more solid particles and colloids were accumulated in the cake layer (Fig. 1b). Interestingly, there were more pores still visible on the surface of the R-UF membrane (Fig. 1c), indicating the effective trapping of suspended and colloidal matter by the bioaugmented filtration. This observation was consistent with the TMP results, in line with less blocking of the UF membrane due to the pre-treatment. Moreover, analysis of the cake layer thickness revealed significant differences between direct UF and R-UF processes. The cake layer thickness on direct UF and R-UF membranes was 2.55 ± 0.04 μm and 135 ± 13 nm, respectively (Fig. 1d-1e). The cake layer thickness was significantly reduced by 94.7%, demonstrating the bioaugmented filtration effectively mitigated UF membrane fouling.

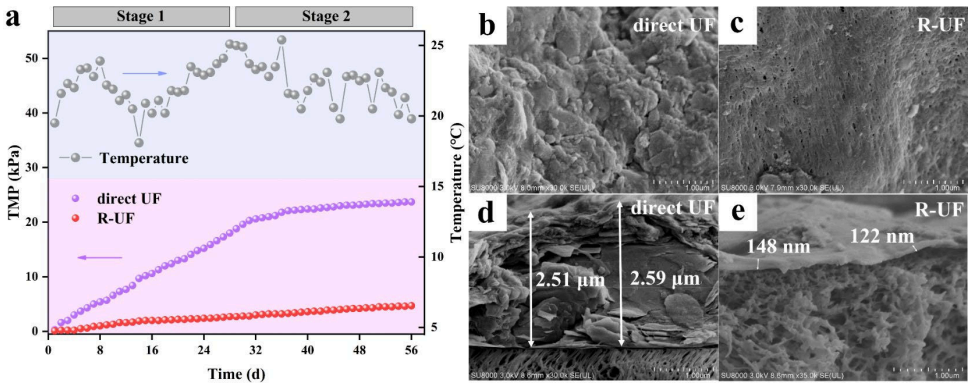

Fig. 1. (a) Direct UF and R-UF processes with data for TMP and influent temperature; SEM images of the membrane plane after the experiment: (b) direct UF process, (c) R-UF process; SEM images revealing the cake layer thickness on membrane surface for different treatment processes: (d) direct UF process, (e) R-UF process (Note: the related scale bare is 1 μm in Figs. 1b-1e).

3.2 Removal performance of ECs

To investigate the effect of different processes on the removal of ECs, four typical ECs were added to the influent and the concentration of ECs was recorded from the 10th day

of stable device operation. The bioaugmented filtration exhibited a significant removal ability of ATL, achieving an average removal rate of 99.5% (Fig. 2a). Although ATL still existed in the R effluent after operation for 7 days, it was completely removed by the subsequent UF membrane. Additionally, direct UF process had a removal effect on ATL and maintained an average removal rate of 46.2%. The performance of the bioaugmented filtration was different for the other three ECs (CBZ, THP, and SMX, Fig. 2b-2d). In stage 1 (the initial 28 days), the bioaugmented filtration was unable to remove CBZ, while the average removal rates for THP and SMX were 44.8% and 30.6%, respectively. At the same time, the removal rates of THP and SMX by the bioaugmented filtration showed a gradual decline, possibly indicating saturation or reduction of adsorption sites on the manganese sand filter material surface. However, starting from the 44th day, the removal rates of CBZ, THP, and SMX by the bioaugmented filtration increased significantly to 10.3%, 54.9%, and 28.0%, respectively. The removal rate of three ECs (CBZ, THP, and SMX) by the bioaugmented filtration showed a trend of increasing and then decreasing after the 44th day. The concentrations of CBZ, THP, and SMX in the effluent of both the direct UF and R-UF processes remained unchanged, indicating that the UF membrane was ineffective in removing these three ECs.

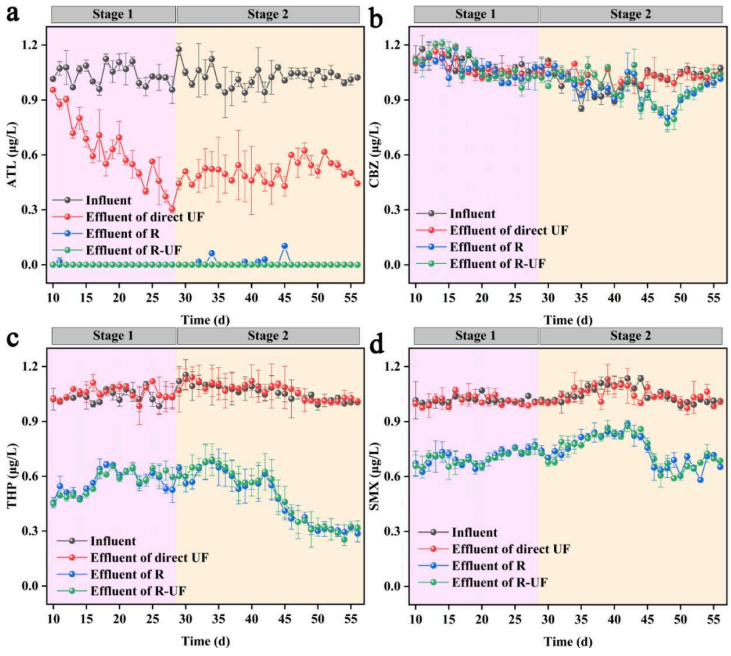

Fig. 2. Concentrations of four ECs in influent and effluent: (a) ATL, (b) CBZ, (c) THP, (d) SMX.

3.3 Effect of bioaugmented filtration and UF on ECs

The extraction ion chromatograms (EIC) and MS spectra for influent, R filter column effluent, and the direct UF effluent were compared by UPLC-Q-TOF-MS. Five possible intermediates in the effluent of the bioaugmented filtration were identified (Fig. 3a-3d, SI Table S2, and SI Fig. S4), while no intermediates of ATL were found in the direct UF effluent (Durán-Álvarez et al., 2024; Kuang et al., 2013; Wei et al., 2024; Zhao et al., 2022b). A previous study has found that water containing ATL is often converted to P1 during degradation, indicating the propensity for ATL degradation via oxidation to produce P1 (Huntscha et al., 2013). P2 was mainly produced by the degradation of CBZ by biological manganese oxides in stage 2 (from day 29 to day 56), indicating the important role of biological manganese oxides in the removal of ECs (Fig. 3b). P3 was generated via the cleavage of the methylene bridge in THP (Fig. 3c) (Kuang et al., 2013). P4-1 and P4-2 were generated by SMX through ring-opening reaction of isoxazole moiety (Fig. 3d) (Luo et al., 2021). An investigation into the distribution characteristics of ATL and PVDF characteristic ion signals in the membrane of direct UF process was performed by ToF-SIMS (Fig. 3e). It was found that the characteristic ion signal peaks of ATL overlapped with PVDF, indicating that ATL was primarily adsorbed by the UF membrane.

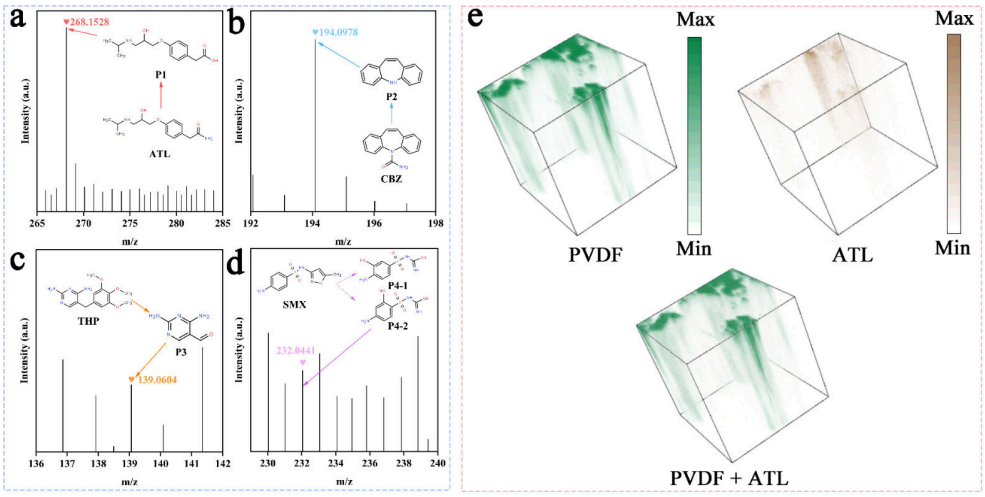

Fig. 3. Mass spectral peaks, m/z, and structural formulae of possible intermediates of four ECs formed by bioaugmented filtration: (a) P1, (b) P2, (c) P3, (d) P4-1, P4-2, (e) 3D reconstruction images of PVDF, ATL, and PVDF + ATL signals in the direct UF process (PVDF + ATL: the superposition of PVDF and ATL characteristic ion signals in the direct UF process)

The assessment of toxicity changes in ECs and their intermediates is crucial for understanding their environmental impact. To understand the characteristics of toxicity changes of ECs and their intermediates, ECOSAR was used to predict the acute and chronic toxicity to aquatic organisms (fish, daphnia, green algae). The toxicity levels could be classified according to the Globally Harmonized System of Classification and Labelling of Chemicals (GHS) (Ortiz de García et al., 2014). It could be stated overall that the intermediates were less toxic than ECs, except for CBZ (SI Fig. S5). The acute and chronic toxicity of the intermediates of ATL, THP, and SMX were significantly reduced after treatment with the bioaugmented filtration, among which the acute toxicity of SMX to daphnia and green algae was reduced from toxic to harmful and from harmful to not harmful, respectively. It showed the potential of bioaugmented filtration in purifying ECs, highlighting its practical application feasibility. It is worth noting that the acute and chronic toxicity of P2 to fish and daphnia were significantly lower than that of CBZ, indicating that P2 still posed ecological risks to some extent.

The predictions from the T.E.S.T. software regarding the bioconcentration factor, developmental toxicity, and mutagenicity of ECs and their intermediates provided further insights into their ecological impact (SI Table S3). With the exception of P3, which was a developmental non-toxicant substance, all other substances were developmental toxicant and mutagenicity negative. However, it is important to note that the bioconcentration factor of P1 significantly decreased compared to ATL, while P2 exhibited a significant increase compared to CBZ. The results were similar to the prediction results of acute and chronic toxicity, highlighting the importance of considering the ecological effects of intermediates of ECs in water treatment.

3.4 Variations of Mn^{2+} concentration and effluent water quality

Manganese is a common contaminant found in drinking water sources, and strict limits were imposed on its permissible concentration levels (Jerroumi et al., 2023). On day 28, the investigation into the removal of Mn^{2+} through direct UF and R-UF processes was initiated by adding 2.5 mg/L of Mn^{2+} to the feed water. On the day 34, the effluent from the direct UF process exhibited a Mn^{2+} concentration of only 0.02

mg/L (SI Fig. S6), which was lower than the standards for drinking water quality in China (GB 5749-2022; the limit of Mn is 0.1 mg/L). Subsequently, stable removal of Mn^{2+} by direct UF process could be achieved, which was similar to the previous report that the UF membrane operated for a long time could remove Mn^{2+} (Chen et al., 2022). Additionally, the bioaugmented filtration, inoculated with manganese-oxidizing bacteria QJX-1, could completely remove Mn^{2+}. The combined action of QJX-1-mediated oxidation of Mn^{2+} and the adsorption capabilities of manganese sand ensured a stable removal effect on the sudden increase of Mn^{2+} in the micro-polluted water source. According to the influent and effluent results of 39 test items on the day 56, both direct UF and R-UF processes could effectively remove the added Mn^{2+}, the aerobic bacteria count, and turbidity (SI Table S4). The water quality of the effluent met the standards for drinking water quality in China (GB 5749-2022, SI Text S1).

4. Discussions

4.1 Removal mechanism of ECs

ECs have a variety of physical properties, including molecular weight, polarity, solubility, and partition coefficient, which affect their environmental recalcitrance and also their associated removal mechanisms in the system (Nguyen et al., 2021).

ECs were mainly removed by the bioaugmented filtration through adsorption, oxidation, and microbial biodegradation. The biological manganese oxides were formed by inoculating manganese-oxidizing bacteria in stage 2 (from day 29 to day 56), resulting in the increase of removal rates of three types ECs (CBZ, THP, and SMX) by increasing the adsorption and oxidation. Mn coating density increased by 7.4% after 56 days operation (SI Fig. S10), which was due to the continuous deposition of biological manganese oxides on manganese sand by manganese-oxidizing bacteria. Since CBZ is difficult to be biodegraded and the effective binding sites of the manganese sand and biological manganese oxide become saturated, the removal rate of CBZ by bioaugmented filtration decreased accordingly starting from day 49. Therefore, it clearly showed that the bioaugmented filtration system constructed by inoculating

manganese-oxidizing bacteria can effectively treat the water source contaminated by manganese and ECs.

Metagenomic analysis of manganese sand before and after the operation revealed the distribution characteristics of microorganisms at the phylum and genus levels, clarifying which microorganisms were effective in ECs removal (Fig. 4). *Pseudomonadota*, *Planctomycetota*, *Nitrospirota*, *Chloroflexota*, *Actinomycetota*, *Acidobacteriota*, and *Bacteroidota* were predominant microbes and collectively accounted for more than 77% of the total population. *Nitrospirota* is a widely reported nitrifying bacterium that may contribute to the biodegradation of THP (Mosley et al., 2024). In addition, a previous study reported that *Bacteroidota* could biodegrade SMX by mineralizing sulphonamide (Wen et al., 2022). The analysis results at the genus level confirmed the existence of *Nitrosomonas*, which was related to the degradation of ATL into P1 (Xu et al., 2017).

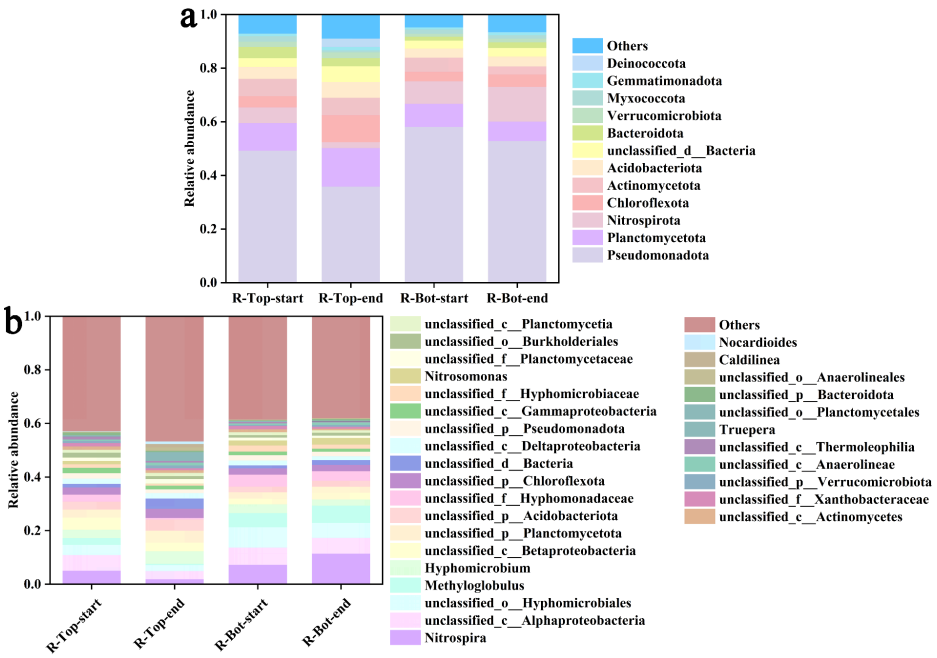

Fig. 4. The relative abundance of bacteria (a) phylum (>0.01), (b) genus (>0.01) on top and bottom manganese sand before and after the experiment (R-Top-start and R-Top-end represent the top manganese sand before and after the experiment, respectively. R-Bot-start and R-Bot-end represent the bottom manganese sand before and after the experiment, respectively).

For UF membrane, due to the large pore size of the membrane and the high logP values of CBZ (3.93), THP (0.38), and SMX (0.89) (Zhao et al., 2022a), which are commonly

used parameters to characterize the hydrophilicity and lipophilicity of ECs, UF was unable to remove these three ECs even after 56 days operation. ATL is a relatively hydrophilic pollutant with a logP value of 0.1 (Zhao et al., 2022a). It should be noted that the PVDF UF membrane used in this work also exhibited a certain hydrophilicity (the contact angle of fresh membrane was 46.6 ± 1.6 °, SI Text S2). Therefore, ATL was more easily adsorbed on membrane surface and within membrane pores.

4.2 Characterization of biofouling in cake layer

It has been demonstrated that cake layer dominates UF membrane fouling, particularly after long-term operation (Wu et al., 2022). Analysis of biological, organic, and inorganic foulant compositions on the fouled membrane surface is shown in SI Text S3. Due to the presence of various microorganisms in feed water and effluent of bioaugmented filtration, analyzing biofouling is crucial for maintaining the stable operation of UF membranes and ensuring the safety of effluent water quality. The sequencing analysis of 16S rRNA and 18S rRNA shed light on the impact of pre-treatment with the bioaugmented filtration on the microbial diversity of the biofilm formed on membrane surface. The Alpha diversity index of the bacterial community in the UF membrane indicated that the bioaugmented filtration effectively reduced the Ace and Chao indices of the R-UF process (SI Fig. S14a-S14b). The results indicated that the bacterial community richness in the direct UF process was higher. In addition, the higher Shannon index and lower Simpson index of the direct UF process indicated a more diverse bacterial community (SI Fig. S14c-S14d). Considering the analysis of SI Text S3, Fig. S12c and S12f, it could be inferred that the bioaugmented filtration not only reduced the biomass on the UF membrane but also decreased the richness and diversity of its bacterial community. This reduction was beneficial for mitigating the UF membrane fouling for the combined process (R-UF).

To reveal the effect of bioaugmented filtration on microbial community structure in biofouling of UF, the Venn diagram of direct UF and R-UF processes and the relative abundance of microorganisms were further compared. The Venn diagram illustrates the comparison of the number of common and unique amplicon sequence variants (ASVs)

between the direct UF and R-UF processes (Fig. 5a). The direct UF process had 3210 ASVs, while the R-UF process had 1522 ASVs. Additionally, there were 139 ASVs shared between the two groups of samples, indicating that the bioaugmented filtration influenced the bacterial diversity of the R-UF process. At the phylum level, the main bacterial groups in both direct UF and R-UF processes were *Proteobacteria, Verrucomicrobiota, Firmicutes, Chloroflexi*, and *Planctomycetota*, collectively accounting for over 88.0% of the total relative abundance (Fig. 5b). Among these, *Proteobacteria* were the most abundant in both types of UF membranes, with the relative abundance in the direct UF process approximately 11.3% higher than that in the R-UF process. In addition, the relative abundance of *Verrucomicrobiota* in the R-UF process (31.2%) was significantly higher compared to the direct UF process (6.0%). The relative abundances of *Firmicutes* and *Chloroflexi* in the direct UF process reached 13.3% and 11.1%, respectively, whereas in the R-UF process, these were only 3.3% and 3.9%, respectively.

The relative abundance of different bacterial genera in the UF membrane provided further insights into the observed differences (Fig. 5c). In the direct UF process, *Bacillus* (12.8%, belonging to *Firmicutes*) and *Hyphomicrobium* (13.8%, belonging to *Proteobacteria*) were prominent genera with high relative abundances. *Bacillus*, a common potential pathogenic found in biofilm samples (Ehling-Schulz et al., 2019), and *Hyphomicrobium* associated with manganese oxidation and deposition (Cerrato et al., 2010), likely contributed to the ability of the direct UF process to remove Mn^{2+} (SI Fig. S6). This introduction of Mn^{2+} potentially influenced the structure and composition of the biofilter cake layer on UF membrane surface, resulting in a slow TMP growth rate of direct UF process in stage 2 (from day 29 to day 56) (Tang et al., 2021). In the R-UF process, the relative abundance of *Bacillus* and *Hyphomicrobium* decreased notably to 3.2% and 1.7%, respectively. Conversely, *norank_f__Methylacidiphilaceae* (18.5%, belonging to *Verrucomicrobiota* and *Methylacidiphilaceae*) and *norank_f__norank_o__norank_c__Planctomycetes* (7.9%, belonging to *Planctomycetota* and *Planctomycetes*) were more prevalent on the R-UF membrane.

According to the bacterial analysis of the manganese sand, two bacteria might mainly come from the effluent of the R filter column (Fig. 4). As revealed in a previous study that the family *Methylacidiphilaceae* could use simple carbon substrates as carbon sources (Awala et al., 2023), potentially aiding in reducing organic fouling. Moreover, *Planctomycetes* were able to efficiently metabolize NO_3^- and NH_4^+ (Zheng et al., 2024), which could be conducive to dealing with nitrogen-polluted water sources. The analysis of eukaryotic communities was presented in SI Text S4. Bioaugmented filtration was demonstrated a remarkable efficacy in capturing the majority of algae and metazoan, thereby significantly mitigating biological fouling.

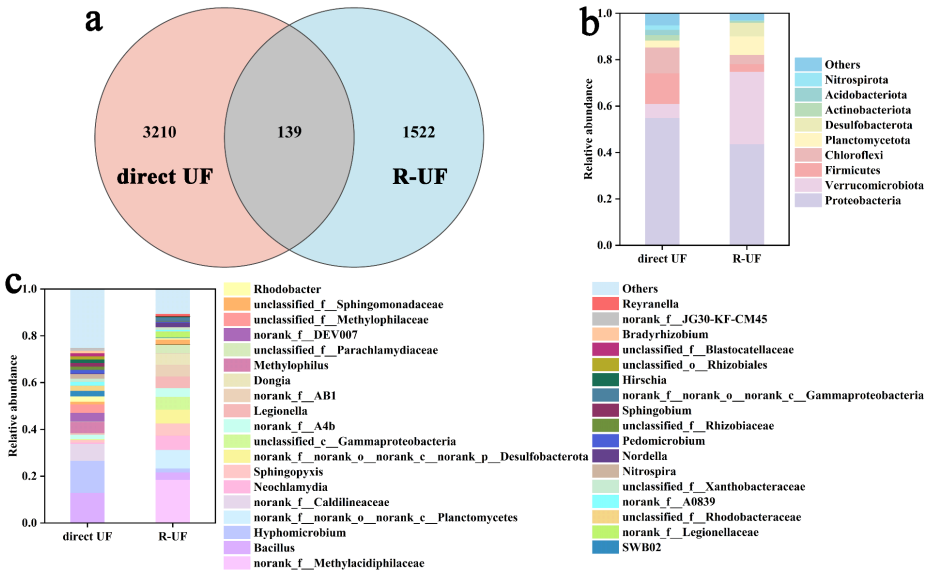

Fig. 5. Bacteria on UF membrane (a) Veen diagram of ASV level, (b) phylum level (> 0.01) relative abundance, (c) genus level (> 0.01) relative abundance.

4.3 Characterization of organic foulants in cake layer

Due to the presence of natural organic matter in river water and the inevitable secretion of extracellular polymeric substances by microorganisms on membrane surface, further investigation on the characteristics of organic pollution in the cake layer is necessary. Organic matter was initially extracted from the surface of the UF membrane. Subsequent analyses, including Excitation-Emission-Matrix (EEM) spectra analysis, polysaccharide and protein determination, and SEC-OCD analysis, were conducted (Fig. 6). The EEM spectra of both direct UF and R-UF processes revealed that the membrane surfaces were primarily fouled by tyrosine, tryptophan, and soluble

microbial byproduct-like materials (Fig. 6a-6b). The calculated $\Phi_{i,n}$ values for direct UF and R-UF processes were found to be closely similar (Fig. 6c), indicating that similarity in the fluorescence organic matter fouling on the membrane surface. Quantitative determination of polysaccharide and protein concentrations indicated that higher levels of polysaccharide (4.02 ± 0.65 μg/mg) and protein (0.23 ± 0.02 μg/mg) on the surface of the direct UF process was observed compared to polysaccharide (3.46 ± 0.52 μg/mg) and protein (0.13 ± 0.04 μg/mg) on the membrane surface of R-UF process (Fig. 6d). SEC-OCD results further revealed the accumulation of more biopolymers (BP) and fulvic-like acids (FA) on the membrane of the direct UF process (Fig. 6e). The results demonstrated that the BP was effectively removed by bioaugmented filtration, such as 13.9% of the polysaccharides and 43.5% of the proteins, thereby mitigating organic fouling on UF membrane surface. The similarity of pore fouling was relatively high; for additional insights into membrane pore fouling, refer to SI Text S5.

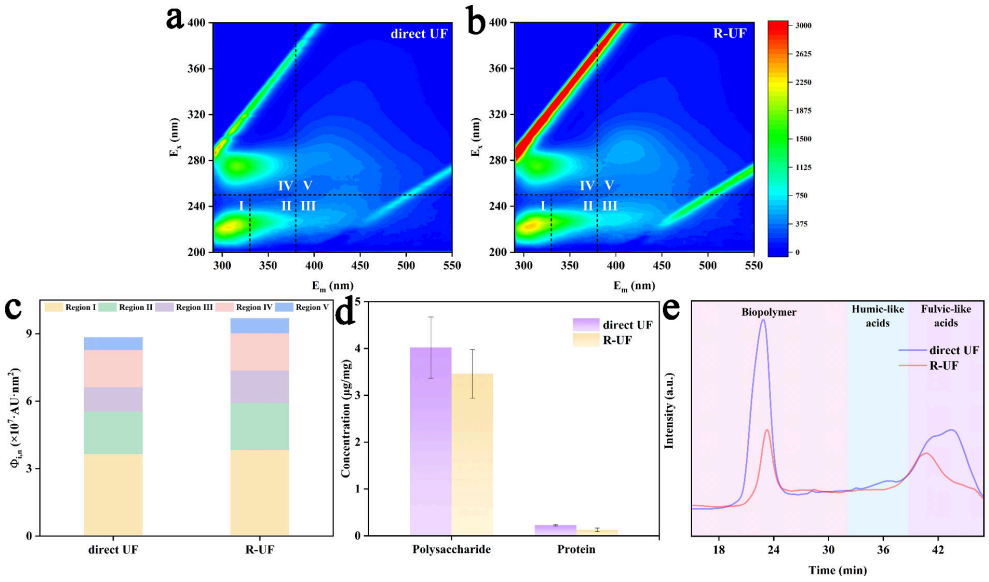

Fig. 6. Analysis of membrane surface fouling: EEM of (a) direct UF, (b) R-UF, (c) $\Phi_{i,n}$, $\Phi_{T,n}$, (d) determination of polysaccharide and protein concentration, (e) SEC-OCD.

4.4 Characterization of inorganic components 3D distribution in cake layer

The accumulation of inorganic pollutants, such as solid particles, on the surface and within the pores of UF membranes can indeed influence membrane performance. The depth profile and 3D distribution of inorganic components and PVDF characteristic ion

signals of UF membrane were analyzed by ToF-SIMS. The relative intensity of signals of different substances is related to their mass concentration. Since the sputtering speed was stable, the depth profile could reflect the content of different substances at different sputtering depths with the increase of sputtering time. In the depth analysis diagram of the cake layer for R-UF process, the signals of inorganic elements (Ca, Mg, Si, and Al) were decreased rapidly with increasing sputtering time and reached the lowest point at 215.6 s (Fig. 7a). Concurrently, the signal of PVDF began to rise. Due to the positive correlation between the sputtering time and the distance of the depth analysis, it meant that the depth analysis had reached the interface between the cake layer and the UF membrane. The 3D distribution characteristics of inorganic elements and PVDF in the area range of 100 μm × 100 μm could be more intuitively observed through 3D reconstruction images (Fig. 7b-7c). The elements on the membrane surface of the R-UF process were analyzed by XPS. Due to the limited detection range of XPS (approximately 10 nm in the depth of the sample) (Sari and Chellam, 2016), no signals for Mg and Al elements were detected. Based on the analysis of Ca 2p and Si 2p (Fig. 7d-7e), it was found that the upper and middle layers of the R-UF process were composed of $CaCO_3$ and SiO_2 (Alfonsetti et al., 1993; Zhang et al., 2018).

To analyze the primary inorganic pollutants in the Yongding River, the ultrafiltration membrane was employed to treat the river water directly (SI Method S6). According to the spectra of Mg 1s and Al 2p, MgO and Al_2O_3 were the primary inorganic fouling corresponding to the Mg and Al elements in the cake layer (Fig. 7f-7g) (Bhardwaj et al., 2019; Kim et al., 1994). It indicated that MgO and Al_2O_3 were predominantly distributed in the middle and lower cake layers for R-UF process. 3D analysis of inorganic composition within cake layer for direct UF process is presented in SI Text S6. Combined with Fig.7b-7c, SI Table S5 and SI Fig. S18, it was evident that bioaugmented filtration effectively alleviated UF inorganic fouling by intercepting $CaCO_3$, SiO_2, MgO and Al_2O_3. These findings provide valuable insights into the composition and distribution of inorganic pollutants within the UF membrane, facilitating a better understanding of membrane fouling mechanisms and potential

mitigation strategies for improving filtration performance.

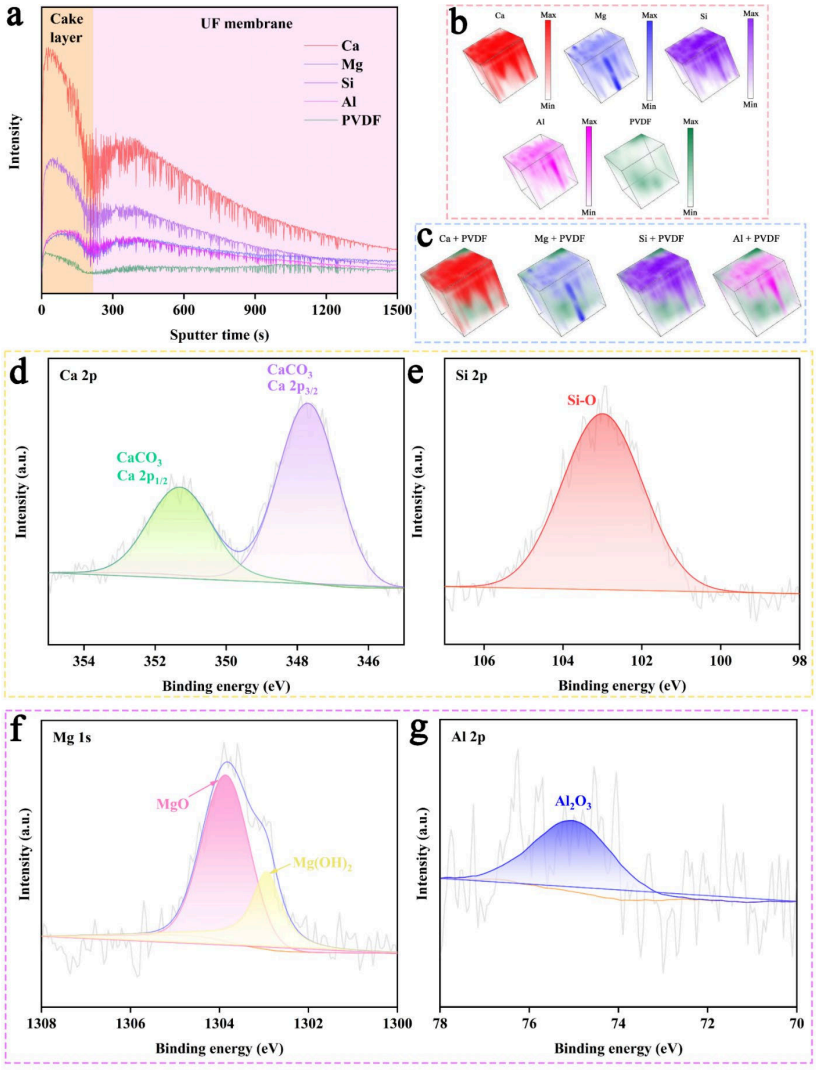

Fig. 7. (a) ToF-SIMS depth profiles of R-UF, (b) 3D reconstructed images of inorganic elements and PVDF, (c) 3D reconstructed images of inorganic elements combined with PVDF (the combination of inorganic elements and PVDF represent the superposition of inorganic elements and PVDF characteristic ion signals), XPS spectrum of R-UF membrane at the end of continuous operation: (d) Ca 2p, (e) Si 2p, XPS spectra of the cake layer after direct UF experiment of Yongding River: (f) Mg 1s, (g) Al 2p.

5. Conclusions

The application of bioaugmented filtration as a membrane filtration pretreatment provides a promising approach to reduce membrane fouling and enhance the synergistic removal of ECs. This study confirmed that the bioaugmented filtration could not only remove organic matters and reduce biodiversity characteristics but also remove

inorganic pollutants and alter their distribution characteristics in the cake layer. Consequently, the TMP of the direct UF process was 5 times that of the combined process. It is worth noting that the common four ECs (ATL, CBZ, THP, and SMX) were mainly removed by the bioaugmented filtration, and ATL was synergistically totally removed by the combined process due to the enhanced adsorption by UF membrane. Furthermore, toxicity prediction elucidated that the intermediates of ATL, THP, and SMX, which were produced by the degradation of the bioaugmented filtration, were significantly less toxic than the parent compounds. Compared with CBZ, the developmental toxicity and mutagenicity of CBZ intermediate were significantly reduced. In this work, as a low-carbon, cost-effective water treatment technology, bioaugmented filtration, can effectively mitigate UF membrane fouling and combine with UF to remove ECs, particularly ATL. These findings will promote the practical application of low-carbon and few-chemical water purification technologies.

CRediT authorship contribution statement

Tingming Ye: Writing – original draft, Visualization, Methodology, Investigation, Formal analysis. **QingJi Wang**: Formal analysis, Funding acquisition. **Jing Qi**: Data curation, Formal analysis. **Baiwen Ma**: Writing – review & editing, Formal analysis, Funding acquisition, Supervision. **Tao Lyu**: Writing – review & editing. **Chengzhi Hu**: Writing – review & editing, Project administration. **Mathias Ulbricht**: Writing – review & editing, Supervision. **Huijuan Liu**: Conceptualization, Writing – review & editing, Funding acquisition, Data curation, Supervision.

Declaration of Competing Interest

The authors declare that they have no known competing financial interests or personal relationships that could have appeared to influence the work reported in this paper.

Data availability statement

The raw sequencing data has been deposited in https://www.cncb.ac.cn/ (CRA019046).

Acknowledgements

This work was financially supported by the National Natural Science Foundation of

China (52322001, 52388101, 52070183), the Program of the Excellent Youth Innovation Promotion Association of the Chinese Academy of Sciences (Y2023010), and the China National Petroleum Corporation (2023ZZ1305).

References

Ajaz, S., Hassan, A.A., Michael, R.N. and Leusch, F.D.L. 2024. Removal of organic micropollutants in biologically active filters: a systematic quantitative review of key influencing factors. Journal of Environmental Management 353.

Alfonsetti, R., Lozzi, L., Passacantando, M., Picozzi, P. and Santucci, S. 1993. XPS studies on SiO_x thin-films. Applied Surface Science 70-1, 222-225.

Andrews, R.C., Taylor-Edmonds, L. and Azzeh, J. 2015. Engineered biofiltration for ultrafiltration fouling mitigation and disinfection by-product precursor control. Water Supply 15(1), 124-133.

Awala, S., Gwak, J.-H., Kim, Y., Seo, C., Strazzulli, A., Kim, S.-G. and Rhee, S.-K. 2023. Methylacidiphilum caldifontis gen. nov., sp. nov., a thermoacidophilic methane-oxidizing bacterium from an acidic geothermal environment, and descriptions of the family Methylacidiphilaceae fam. nov. and order Methylacidiphilales ord. nov. International Journal of Systematic and Evolutionary Microbiology 73.

Bai, X., Samari-Kermani, M., Schijven, J., Raoof, A., Dinkla, I.J.T. and Muyzer, G. 2024. Enhancing slow sand filtration for safe drinking water production: interdisciplinary insights into Schmutzdecke characteristics and filtration performance in mini-scale filters. Water Research 262.

Bai, Y., Yang, T., Liang, J. and Qu, J. 2016. The role of biogenic Fe-Mn oxides formed in situ for arsenic oxidation and adsorption in aquatic ecosystems. Water Research 98, 119-127.

Bhardwaj, V., Chen, K.M., Tseng, Y.C. and Chatterjee, R. 2019. Study of Al interdiffusion in ultrathin β-Ta/Co_2FeAl/MgO heterostructures for enhanced spin-orbit torque. Physica B-Condensed Matter 574.

Cerrato, J.M., Falkinham, J.O., 3rd, Dietrich, A.M., Knocke, W.R., McKinney, C.W. and Pruden, A. 2010. Manganese-oxidizing and -reducing microorganisms isolated from biofilms in chlorinated drinking water systems. Water Research 44(13), 3935-3945.

Chen, R., Zhang, H., Wang, J., Xu, D., Tang, X., Gong, W. and Liang, H. 2022. Insight into the role of biogenic manganese oxides-assisted gravity-driven membrane filtration systems toward emerging contaminants removal. Water Research 224.

Chen, Y., Li, M., Gao, W., Guan, Y., Hao, Z. and Liu, J. 2024. Occurrence and risks of pharmaceuticals, personal care products, and endocrine-disrupting compounds in Chinese surface waters. Journal of Environmental Sciences 146, 251-263.

Dirani, L., Ayoub, G.M., Malaeb, L. and Zayyat, R.M. 2024. A review on the occurrence of per- and polyfluoroalkyl substances in the aquatic environment and treatment trends for their removal. Journal of Environmental Chemical Engineering 12(5).

Durán-Álvarez, J.C., Cortés-Lagunes, S., Mahjoub, O., Serrano-Lázaro, A., Garduño-Jiménez, A. and Zanella, R. 2024. Tapping the Tunisian sunlight's potential to remove pharmaceuticals in tap water and secondary effluents: A comparison of Ag_2O/TiO_2 and BiOI photocatalysts and toxicological insights. Separation and Purification Technology 335.

Ehling-Schulz, M., Lereclus, D. and Koehler, T.M. 2019. The Bacillus cereus group: Bacillus species

with pathogenic potential. Microbiology Spectrum 7(3).

Furgal, K.M., Meyer, R.L. and Bester, K. 2015. Removing selected steroid hormones, biocides and pharmaceuticals from water by means of biogenic manganese oxide nanoparticles in situ at ppb levels. Chemosphere 136, 321-326.

Huang, Y., Li, H., Zhou, Q., Li, A.M., Shuang, C.D., Xian, Q.M., Xu, B. and Pan, Y. 2018. New phenolic halogenated disinfection byproducts in simulated chlorinated drinking water: identification, decomposition, and control by ozone-activated carbon treatment. Water Research 146, 298-306.

Huck, P.M., Anderson, W.B., Van Dyke, M.I., Jin, X., Ndiongue, S. and Rahman, I. 2014. Fouling of low-pressure membranes during drinking water treatment: effect of NOM components and biofiltration pretreatment. Water Supply 14(3), 453-460.

Huntscha, S., Rodriguez Velosa, D.M., Schroth, M.H. and Hollender, J. 2013. Degradation of polar organic micropollutants during riverbank filtration: complementary results from spatiotemporal sampling and push–pull tests. Environmental Science & Technology 47(20), 11512-11521.

Jerroumi, S., Amarine, M. and Gourich, B. 2023. Technological trends in manganese removal from groundwater: A review. Journal of Water Process Engineering 56.

Ji, W.-X., Tian, Y.-C., Li, A.-m., Gu, X.-M., Sun, H.-F., Cai, M.-H., Shen, S.-Q., Zuo, Y.-T. and Li, W.-T. 2022. Unravelling relationships between fluorescence spectra, molecular weight distribution and hydrophobicity fraction of dissolved organic matter in municipal wastewater. Chemosphere 308.

Kim, Y.C., Park, H.H., Chun, J.S. and Lee, W.J. 1994. Compositional and structural-analysis of aluminum-oxide films prepared by plasma-enhanced chemical-vapor-deposition. Thin Solid Films 237(1-2), 57-65.

Kuang, J., Huang, J., Wang, B., Cao, Q., Deng, S. and Yu, G. 2013. Ozonation of trimethoprim in aqueous solution: identification of reaction products and their toxicity. Water Research 47(8), 2863-2872.

Liu, M., Graham, N., Xu, L., Zhang, K. and Yu, W. 2023. Bubbleless aerated-biological activated carbon as a superior process for drinking water treatment in rural areas. Water Research 240.

Luo, M., Zhou, H., Zhou, P., Lai, L., Liu, W., Ao, Z., Yao, G., Zhang, H. and Lai, B. 2021. Insights into the role of in-situ and ex-situ hydrogen peroxide for enhanced ferrate(VI) towards oxidation of organic contaminants. Water Research 203.

Manoli, K., Li, R.B., Kim, J., Feng, M.B., Huang, C.H. and Sharma, V.K. 2022. Ferrate(VI)-peracetic acid oxidation process: rapid degradation of pharmaceuticals in water. Chemical Engineering Journal 429.

Marques, R.Z., Oliveira, P.G.D., Barbato, M.L., Kitamura, R.S.A., Maranho, L.T., Brito, J.C.M., Nogueira, K.d.S., Juneau, P. and Gomes, M.P. 2024. Green solutions for antibiotic pollution: assessing the phytoremediation potential of aquatic macrophytes in wastewater treatment plants. Environmental Pollution 357.

Meng, S., Wang, R., Zhang, K., Meng, X., Xue, W., Liu, H., Liang, D., Zhao, Q. and Liu, Y. 2020. Transparent exopolymer particles (TEPs)-associated protobiofilm: a neglected contributor to biofouling during membrane filtration. Frontiers of Environmental Science & Engineering 15(4).

Mohammed, A.B., Raju, A.K.S., Lee, J., Oh, Y.M. and Jeong, S. 2021. Non-chemical biofouling mitigation systems for seawater cooling tower using granular activated carbon biofiltration and ultrafiltration. Journal of Environmental Chemical Engineering 9(6).

Mosley, O.E., Gios, E. and Handley, K.M. 2024. Implications for nitrogen and sulphur cycles: phylogeny and niche-range of Nitrospirota in terrestrial aquifers. ISME Communications 4(1).

Nguyen, P.Y., Carvalho, G., Reis, M.A.M. and Oehmen, A. 2021. A review of the biotransformations of priority pharmaceuticals in biological wastewater treatment processes. Water Research 188.

Ortiz de García, S.A., Pinto Pinto, G., García-Encina, P.A. and Irusta-Mata, R. 2014. Ecotoxicity and environmental risk assessment of pharmaceuticals and personal care products in aquatic environments and wastewater treatment plants. Ecotoxicology 23(8), 1517-1533.

Palaniswamy, S., Nevala, L., Pesonen, P., Rautio, A., Jarvelin, M.-R., Abass, K. and Charles, D. 2024. Environmental contaminants in Arctic human populations: trends over 30years. Environment International 189, 108777-108777.

Qu, J.H. and Chen, J.P. 2024. Pathways toward a pollution-free planet and challenges. Frontiers of Environmental Science & Engineering 18(6).

Ren, C.-Y., Xu, Q.-J., Alvarez, P.J.J., Zhu, L. and Zhao, H.-P. 2023. Simultaneous antibiotic removal and mitigation of resistance induction by manganese bio-oxidation process. Water Research 244.

Sari, M.A. and Chellam, S. 2016. Reverse osmosis fouling during pilot-scale municipal water reuse: evidence for aluminum coagulant carryover. Journal of Membrane Science 520, 231-239.

Tang, X., Zhu, X., Huang, K., Wang, J., Guo, Y., Xie, B., Li, G. and Liang, H. 2021. Can ultrafiltration singly treat the iron- and manganese-containing groundwater? Journal of Hazardous Materials 409.

Therdkiattikul, N., Kidkhunthod, P., Chaiprapa, J., Limpiyakorn, T., Khan, E., Ratpukdi, T. and Siripattanakul-Ratpukdi, S. 2023. Initial stage of innovative cell-entrapped biofilter start-up for removal of manganese in water: treatment performance, manganese speciation, and microbial community. Journal of Water Process Engineering 54.

Urtiaga, A.M., Pérez, G., Ibáñez, R. and Ortiz, I. 2013. Removal of pharmaceuticals from a WWTP secondary effluent by ultrafiltration/reverse osmosis followed by electrochemical oxidation of the RO concentrate. Desalination 331, 26-34.

Wang, X., Jing, J., Zhou, M. and Dewil, R. 2023. Recent advances in H_2O_2-based advanced oxidation processes for removal of antibiotics from wastewater. Chinese Chemical Letters 34(3).

Wei, Y., Hu, D., Ye, C., Zhang, H., Li, H. and Yu, X. 2023. Drinking water quality & health risk assessment of secondary water supply systems in residential neighborhoods. Frontiers of Environmental Science & Engineering 18(2).

Wei, Y., Liu, Y., Wang, T., Zhang, G., Yang, L., He, C., Xiong, Z., Pan, Z. and Lai, B. 2024. N, S co-doped porous carbon to accelerate Fe^{3+}/Fe^{2+} redox cycle for peroxymonosulfate activation. Separation and Purification Technology 328.

Wen, H., Zhu, H., Yan, B., Bañuelos, G., Shutes, B., Wang, X., Cao, S., Cheng, R. and Tian, L. 2022. High removal efficiencies of antibiotics and low accumulation of antibiotic resistant genes obtained in microbial fuel cell-constructed wetlands intensified by sponge iron. Science of The Total Environment 806.

Wu, S., Hua, X., Ma, B., Fan, H., Miao, R., Ulbricht, M., Hu, C. and Qu, J. 2021. Three-dimensional analysis of the natural-organic-matter distribution in the cake layer to precisely reveal ultrafiltration fouling mechanisms. Environmental Science & Technology 55(8), 5442-5452.

Wu, S., Lu, C., Ma, B., Liu, R., Hu, C., Ulbricht, M. and Qu, J. 2022. Long-term direct ultrafiltration without chemical cleaning for purification of micro-polluted water in rural regions: feasibility and application prospects. Chemical Engineering Journal 443.

Xu, L., Zhou, Z., Graham, N.J.D., Liu, M. and Yu, W. 2021. Enhancing ultrafiltration performance by gravity-driven up-flow slow biofilter pre-treatment to remove natural organic matters and biopolymer foulants. Water Research 195.

Xu, Y., Radjenovic, J., Yuan, Z. and Ni, B.-J. 2017. Biodegradation of atenolol by an enriched nitrifying sludge: Products and pathways. Chemical Engineering Journal 312, 351-359.

Yang, Y., Liu, J.Z., Zhang, S., Wang, J.J., Li, W.Y. and Gu, J.L. 2024. Enhanced biofiltration coupled with ultrafiltration process in marine recirculating aquaculture system: fast start-up of nitrification and long-term performance. Separation and Purification Technology 335.

Ye, T.M., Liu, H.J., Qi, W.X. and Qu, J.H. 2023. Removal of pharmaceutical in a biogenic/chemical manganese oxide system driven by manganese-oxidizing bacteria with humic acids as sole carbon source. Journal of Environmental Sciences 126, 734-741.

Zhang, M.J., Hong, H.C., Lin, H.J., Shen, L.G., Yu, H.Y., Ma, G.C., Chen, J.R. and Liao, B.Q. 2018. Mechanistic insights into alginate fouling caused by calcium ions based on terahertz time-domain spectra analyses and DFT calculations. Water Research 129, 337-346.

Zhao, J., Fang, S., Liu, G., Qi, W., Bai, Y., Liu, H. and Qu, J. 2022a. Role of ammonia-oxidizing microorganisms in the removal of organic micropollutants during simulated riverbank filtration. Water Research 226.

Zhao, J., Fang, S., Qi, W., Liu, H. and Qu, J. 2022b. Do NH_4^+-N and AOB affect atenolol removal during simulated riverbank filtration? Chemosphere 301.

Zhao, Q.Y., Zhang, Y.Y., Li, X.W., Hu, X.D., Huang, R., Xu, J.X., Yin, Z.L., Gu, X.J., Xu, Y.C., Yin, J.B., Zhou, Q., Li, A.M. and Shi, P. 2024. Evaluating a river's ecological health: a multidimensional approach. Environmental Science and Ecotechnology 21.

Zheng, R., Wang, C., Liu, R., Cai, R. and Sun, C. 2024. Physiological and metabolic insights into the first cultured anaerobic representative of deep-sea Planctomycetes bacteria. Elife 12.

Zhou, J., Wang, D., Ju, F., Hu, W., Liang, J., Bai, Y., Liu, H. and Qu, J. 2022. Profiling microbial removal of micropollutants in sand filters: biotransformation pathways and associated bacteria. Journal of Hazardous Materials 423.

DSPACE

https://dspace.org/

Exploring advanced and sustainable bioaugmentation-enhanced ultrafiltration processes for the removal of emerging contaminants

Ye, Tingming; Wang, QingJi; Qi, Jing; Ma, Baiwen; Lyu, Tao ...

2025-03-01
Elsevier
https://doi.org/10.1016/j.memsci.2025.123784
Ye T, Wang Q, Qi J, et al., (2025) Exploring advanced and sustainable bioaugmentation-enhanced ultrafiltration processes for the removal of emerging contaminants. Journal of Membrane Science, Volume 720, March 2025, Article number 123784

Downloaded from a DSpace repository. https://dspace.org/